White Rose Research Online

eprints@whiterose.ac.uk
https://eprints.whiterose.ac.uk
Universities of Leeds, Sheffield and York

Deposited via The University of Sheffield.

White Rose Research Online URL for this paper:
https://eprints.whiterose.ac.uk/id/eprint/111843/

Version: Supplemental Material

Article:
Gillespie, P. and Martsinovich, N. (2017) Electronic Structure and Charge Transfer in the TiO2 Rutile (110)/Graphene Composite Using Hybrid DFT Calculations. Journal of Physical Chemistry C, 121 (8). pp. 4158-4171. ISSN: 1932-7447

https://doi.org/10.1021/acs.jpcc.6b12506

This document is the Accepted Manuscript version of a Published Work that appeared in final form in Journal of Physical Chemistry C, copyright © American Chemical Society after peer review and technical editing by the publisher. To access the final edited and published work see https://doi.org/10.1021/acs.jpcc.6b12506.

Reuse
Items deposited in White Rose Research Online are protected by copyright, with all rights reserved unless indicated otherwise. They may be downloaded and/or printed for private study, or other acts as permitted by national copyright laws. The publisher or other rights holders may allow further reproduction and re-use of the full text version. This is indicated by the licence information on the White Rose Research Online record for the item.

Takedown
If you consider content in White Rose Research Online to be in breach of UK law, please notify us by emailing eprints@whiterose.ac.uk including the URL of the record and the reason for the withdrawal request.

UNIVERSITY OF LEEDS
University of Sheffield
UNIVERSITY of York

Supporting Information for

Electronic Structure and Charge Transfer in the TiO_2 Rutile (110) / Graphene Composite Using Hybrid DFT Calculations

Peter Gillespie and Natalia Martsinovich**

Department of Chemistry, University of Sheffield, Brook Hill, Sheffield, S3 7HF, UK

E-mail: pnogillespie1@sheffield.ac.uk; n.martsinovich@sheffield.ac.uk

Contents

S1. Construction of commensurate unit cells (Tables S1-S6, Figure S1) ...…… p. S2

S2. Strain tests data: band gaps, energies and Fermi level shifts (Table S7) ……..p. S6

S3. Band structures of highly strained graphene (Figure S2) ...……..…….…….....p. S7

S4. Interaction energies in the TiO_2/graphene system (Table S8) ……...…….…….....p. S8

S5. Density of states for the 6-atomic-layer rutile (110)/graphene composite system (Figure S3) ..p. S9

S6. Charge density difference in the rutile (110)/graphene composite system (Figure S4) …...…p. S10

S7. Band structures of the rutile (110) and graphene components (Figure S5)…….……..p. S11

S8. Example of CP2K input file for rutile (110)/graphene system…….....…….……p. S12

S1. Construction of commensurate rutile (110)-graphene unit cells

Construction of this commensurate cell requires unit cells of rutile (110) and graphene. The calculated bulk TiO_2 rutile lattice parameters (obtained from bulk rutile unit cell optimisation using the PBE functional and DZVP basis sets in the CP2K software, with a 3 × 3 × 2 supercell) are a = 4.617 Å, c = 2.995 Å. The values found using the HSE06 functional with triple-zeta polarised basis sets using CRYSTAL14 are very similar: a = 4.579 Å, c = 2.951 Å. Both are in good agreement with the experimental values a = 4.593 Å, c = 2.958 Å.[1] The PBE-optimised bulk cell was used to construct rutile (110) slabs, with cell parameters of the slabs A_{ru} = 6.529 Å and B_{ru} = 2.995 Å.

For graphene, orthorhombic unit cell was used, with lattice parameters A_{gr} = 4.254 Å and B_{gr} = 2.46 Å (both cells are shown in Figure 1 in the main text).

To construct a commensurate unit cell of the rutile (110)/graphene composite, the lowest common multiples of the cell parameters of rutile (110) compared to graphene need to be found. Generally, a n × m extended supercell of rutile (110) is combined with a N × M extended supercell of graphene, where n, m, N, M are integer numbers. The aim is therefore to find such combinations of n with N, and m with M, which lead to the smallest lattice mismatch between TiO_2 and graphene supercells.

Two orientations of the graphene layer with respect to rutile (110) are considered: (i) the A_{gr} (armchair) lattice vector of graphene is parallel to the A_{ru} lattice vector of rutile (110), as in Figure 1 in the main text (results in Tables S1-S3), and (ii) 90° rotation of the graphene layer: the B_{gr} vector (zigzag line) of graphene is parallel to the A_{ru} cell vector of rutile (110) (Figure S1 and Tables S4-S6).

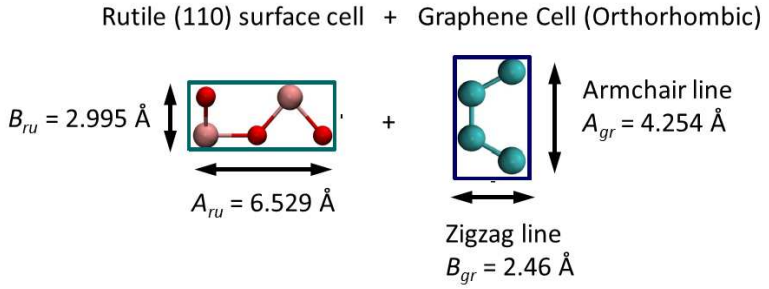

Figure S1. Combining a rutile (110) cell with an orthorhombic graphene cell by orienting the B_{gr} vector (zigzag line) of graphene parallel to the A_{ru} cell vector of rutile (110).

(i) When the A_{gr} (armchair) lattice vector of graphene is parallel to the A_{ru} lattice vector of rutile (110), the dimensions of the composite unit cell are $n_{ru}\,A_{ru} = N_{gr}\,A_{gr}$ (horizontal) and $m_{ru}\,B_{ru} = M_{gr}\,B_{gr}$ (vertical). The combinations of n_{ru} with N_{gr}, and m_{ru} with M_{gr} should be such that $n_{ru}\,A_{ru}$ is as close as possible to $N_{gr}\,A_{gr}$, and $m_{ru}\,A_{ru}$ is as close as possible to $M_{gr}\,A_{gr}$.

To construct commensurate cells, we systematically scan through all possible combinations of n_{ru} with N_{gr}, and m_{ru} with M_{gr}. For each value of n_{ru} from 1 to 15, we find the corresponding value of N_{gr} that gives the smallest difference between $n_{ru}\,A_{ru}$ and $N_{gr}\,A_{gr}$. The same procedure is followed for m_{ru} with M_{gr}.

Tables S1 and S2 summarise the obtained combinations of n_{ru} with N_{gr}, and m_{ru} with M_{gr}, respectively, together with the amount of lattice mismatch (in %) for these combinations. Cells with small mismatch are highlighted in bold. Table S3 shows the number of atoms in the resulting rutile (100)/graphene composite cells based on the best combinations of n_{ru} with N_{gr}, and m_{ru} with M_{gr}.

The smallest-size cell with small lattice mismatch (2.32% and 1.44% in the A and B directions, respectively), is the combination of a 3×6 supercell of graphene with a 2×5 supercell of rutile (110),

[1] J. K. Burdett, T. Hughbanks, G. J. Miller, J. W. Richardson, J. V. Smith, *J. Am. Chem. Soc*. 1987, **109**, 3639–3646.

used in this work (192 atoms when the 6 atomic-layer rutile slab is used, or 252 atoms with the 9 atomic-layer rutile slab) and in the literature.[2] Mismatch below 2% can be achieved only with much larger cell sizes involving over 1000 atoms (Table S3). This much greater computational expense is not expected to greatly improve the accuracy of the interface model (see strain tests, Fig. 2 in the main text and Table S7).

Table S1. Matching the A_{ru} parameter of rutile (110) to the A_{gr} parameter of graphene

n_{ru}	N_{gr}	$n_{ru} \times A_{ru}$, Å	$N_{gr} \times A_{gr}$, Å	Mismatch = $(n_{ru} \times A_{ru}) - (N_{gr} \times A_{gr})$, Å	Mismatch / $(N_{gr} \times A_{gr})$, %	Comments
1	2	6.53	8.51	-1.98	-23.26	
2	**3**	**13.06**	**12.76**	**0.30**	**2.32**	**Best small cell (this work)**
3	5	19.59	21.27	-1.68	-7.91	
4	6	26.12	25.52	0.59	2.32	
5	8	32.65	34.03	-1.39	-4.08	
6	9	39.17	38.29	0.89	2.32	
7	11	45.70	46.79	-1.09	-2.33	
8	12	52.23	51.05	1.18	2.32	
9	**14**	**58.76**	**59.56**	**-0.80**	**-1.33**	**Good match; large cell**
10	15	65.29	63.81	1.48	2.32	
11	**17**	**71.82**	**72.32**	**-0.50**	**-0.69**	**Good match; large cell**
12	18	78.35	76.57	1.78	2.32	
13	**20**	**84.88**	**85.08**	**-0.20**	**-0.24**	**Good match; large cell**
14	21	91.41	89.33	2.07	2.32	
15	**23**	**97.94**	**97.84**	**0.09**	**0.10**	**Good match; large cell**

Table S2. Matching the B_{ru} parameter of rutile (110) to the B_{gr} parameter of graphene

m_{ru}	M_{gr}	$m_{ru} \times B_{ru}$, Å	$M_{gr} \times B_{gr}$, Å	Mismatch = $(m_{ru} \times B_{ru}) - (M_{gr} \times B_{gr})$, Å	Mismatch / $(M_{gr} \times B_{gr})$, %	Comments
1	1	3.00	2.46	0.54	21.75	
2	3	5.99	7.38	-1.39	-18.83	
3	4	8.99	9.84	-0.86	-8.69	
4	**5**	**11.98**	**12.30**	**-0.32**	**-2.60**	**Alternative smaller cell**
5	**6**	**14.98**	**14.76**	**0.22**	**1.46**	**Best small cell (this work)**
6	7	17.97	17.22	0.75	4.36	
7	9	20.97	22.14	-1.18	-5.31	
8	10	23.96	24.60	-0.64	-2.60	
9	**11**	**26.96**	**27.06**	**-0.10**	**-0.39**	**Good match; large cell**
10	12	29.95	29.52	0.43	1.46	
11	13	32.95	31.98	0.97	3.02	
12	15	35.94	36.90	-0.96	-2.60	
13	16	38.94	39.36	-0.42	-1.08	
14	**17**	**41.93**	**41.82**	**0.11**	**0.26**	**Good match; large cell**
15	18	44.93	44.28	0.65	1.46	

[2] A. Du, Y. H. Ng, N. J. Bell, Z. Zhu, R. Amal, S. C. Smith, *J. Phys. Chem. Lett.* 2011, **2**, 894–899.

Table S3. Sizes of rutile (110)/graphene composite cells with small lattice mismatch: $n_{ru} \times m_{ru}$ rutile (110) cells interfaced with $N_{gr} \times M_{gr}$ graphene cells

$n_{ru} \times m_{ru}$	$N_{gr} \times M_{gr}$	Number of atoms (with 6 atomic-layer TiO_2)	Number of atoms (with 9 atomic-layer TiO_2)	Mismatch along *A* and *B*, %
2 × 5	3 × 6	192	252	+2.32% and +1.46%
2 × 9	3 × 11	348	456	+2.32% and -0.39%
2 × 14	3 × 14	540	708	+2.32% and +0.26%
9 × 14	3 × 6	876	1146	-1.33% and +1.46%
9 × 14	3 × 11	1588	2074	-1.33% and -0.39%
9 × 14	3 × 14	2464	3220	-1.33% and +0.26%
15 × 23	3 × 6	1212	1662	+0.10% and +1.46%
15 × 23	3 × 11	2192	3002	+0.10% and -0.39%
15 × 23	3 × 14	3404	4664	+0.10% and +0.26%

(ii) Tables S4 and S5 describe the lattice matching procedure for case (ii), i.e. the orientation of graphene with respect to rutile (110) where the zigzag line of graphene (vector B_{gr}) runs parallel to the A_{ru} cell vector of rutile (110), shown in Figure S1. Here, combinations of n_{ru}, M_{gr}, m_{ru}, A_{gr} should ensure $n_{ru}\, A_{ru} = M_{gr}\, B_{gr}$, and $m_{ru}\, B_{ru} = N_{gr}\, A_{gr}$. We find that commensurability of $n_{ru}\, A_{ru}$ with $M_{gr}\, B_{gr}$ can be achieved already with small supercell extensions, while commensurability of $m_{ru}\, B_{ru}$ with $N_{gr}\, A_{gr}$ requires large supercell extensions.

Cell sizes for the resulting best composite cells are given in Table S6. The smallest commensurate unit cell combines an 8 × 5 supercell of graphene with a 3 × 7 supercell of rutile (110), with the strain of -1.43% and -0.47% to the armchair and zigzag graphene directions, respectively (412 atoms with a 6 atomic layer slab of rutile (110)). An even better match (strain of -0.47% and +0.58% in the armchair and zigzag lines, respectively) can be obtained by combining an 8×7 supercell of graphene with a 3×10 supercell of rutile (110), but the cell size (584 atoms with a 6 atomic layer rutile (110) slab) is too large for practical use, and improvements in quality are expected to be minimal.

Table S4. Matching the A_{ru} parameter of rutile (110) to the B_{gr} parameter of graphene

n_{ru}	M_{gr}	$n_{ru} \times A_{ru}$	$M_{gr} \times B_{gr}$	Mismatch $(n_{ru} \times A_{ru}) - (M_{gr} \times B_{gr})$, Å	Mismatch / $(M_{gr} \times B_{gr})$, %	Comments
1	3	6.53	7.38	-0.85	-11.53	
2	5	13.06	12.30	0.76	6.16	
3	**8**	**19.59**	**19.68**	**-0.09**	**-0.47**	**Best small cell**
4	11	26.12	27.06	-0.94	-3.49	
5	13	32.65	31.98	0.66	2.08	
6	16	39.17	39.36	-0.19	-0.47	
7	19	45.70	46.74	-1.04	-2.22	
8	21	52.23	51.66	0.57	1.11	
9	24	58.76	59.04	-0.28	-0.47	
10	27	65.29	66.42	-1.13	-1.70	
11	29	71.82	71.34	0.48	0.67	
12	32	78.35	78.72	-0.37	-0.47	
13	34	84.88	83.64	1.24	1.48	
14	**37**	**91.41**	**91.02**	**0.39**	**0.42**	**Good match; very large cell**
15	40	97.94	98.40	-0.47	-0.47	

Table S5. Matching the B_{ru} parameter of rutile (110) to the A_{gr} parameter of graphene

m_{ru}	N_{gr}	$m_{ru} \times A_{ru}$	$N_{gr} \times B_{gr}$	Mismatch $(m_{ru} \times B_{ru}) - (N_{gr} \times A_{gr})$, Å	Mismatch / $(N_{gr} \times A_{gr})$, %	Comments
1	1	3.00	4.25	-1.26	-29.60	
2	2	5.99	8.51	-2.52	-29.60	
3	2	8.99	8.51	0.48	5.61	
4	3	11.98	12.76	-0.78	-6.13	
5	4	14.98	17.02	-2.04	-11.99	
6	4	17.97	17.02	0.95	5.61	
7	**5**	**20.97**	**21.27**	**-0.30**	**-1.43**	**Best small cell**
8	6	23.96	25.52	-1.56	-6.13	
9	6	26.96	25.52	1.43	5.61	
10	**7**	**29.95**	**29.78**	**0.17**	**0.58**	**Good match; large cell**
11	8	32.95	34.03	-1.09	-3.19	
12	8	35.94	34.03	1.91	5.61	
13	9	38.94	38.29	0.65	1.70	
14	10	41.93	42.54	-0.61	-1.43	
15	11	44.93	46.79	-1.87	-3.99	

Table S6. Sizes of rutile (110)/graphene composite cells with small lattice mismatch: $n_{ru} \times m_{ru}$ rutile (110) cells interfaced with $M_{gr} \times N_{gr}$ graphene cells: graphene's zigzag direction ($M_{gr} \times B_{gr}$) is parallel to the $n_{ru} \times A_{ru}$ cell vector of rutile (110)

$n_{ru} \times m_{ru}$	$M_{gr} \times N_{gr}$	Number of atoms (with 6 atomic-layer TiO_2)	Number of atoms (with 9 atomic-layer TiO_2)	Mismatch along A_{ru} and B_{ru}, %
3 × 7	8 × 5	412	538	-0.47% and -1.43%
3 × 10	8 × 7	584	764	-0.47% and +0.57%
14 × 7	8 × 5	2504	3386	+0.42% and -1.43%
14 × 10	8 × 7	3556	4816	+0.42% and +0.57%

S2. Strain tests data: band gaps, energies and Fermi level shifts

Table S7. Change in observed band gap, Fermi level and total energy difference relative to fully optimised orthorhombic graphene for each level of applied strain. These data are also presented graphically in Figure 3 of the main text

Strain (%)	Armchair direction			Zigzag direction		
	Band Gap (eV)	Energy Difference (eV)	Fermi Level Shift (eV)	Band Gap (eV)	Energy Difference (eV)	Fermi Level Change (eV)
30	0.013	4.67	-0.73	0.173	5.63	-0.74
25	0.003	4.16	-0.66	0.003	4.39	-0.53
20	0.011	3.10	-0.42	0.002	3.14	-0.40
15	0.006	1.98	-0.33	0.005	1.97	-0.33
10	0.007	0.99	-0.25	0.006	0.98	-0.25
6	0.011	0.39	-0.17	0.007	0.38	-0.17
5	0.001	0.28	-0.15	0.001	0.27	-0.14
4	0.003	0.19	-0.12	0.008	0.18	-0.12
3	0.005	0.11	-0.09	0.008	0.10	-0.09
2	0.004	0.05	-0.06	0.005	0.05	-0.06
1	0.010	0.01	-0.03	0.004	0.01	-0.02
0	0.001	0.00	0.00	0.001	0.00	0.00
-1	0.007	0.01	0.04	0.007	0.01	0.04
-2	0.005	0.04	0.08	0.002	0.05	0.08
-3	0.010	0.10	0.08	0.008	0.11	0.12
-4	0.002	0.18	0.13	0.001	0.20	0.16
-5	0.003	0.29	0.17	0.006	0.31	0.20
-6	0.008	0.43	0.22	0.008	0.46	0.25
-10	0.001	1.34	0.46	0.001	1.39	0.46
-15	0.013	3.30	0.77	0.006	3.42	0.78
-20	0.009	6.39	1.12	0.008	6.59	1.28

The accuracy of our estimated band gaps is limited by the density of the **k**-point sampling. We evaluate the uncertainly in our band gaps as ≤0.01 eV (as the difference between the conduction band energies at the Dirac point and at the next k-point). This uncertainty is similar to those reported in earlier studies: 0.01 eV[3] or 0.0003-0.04 eV depending in the k-point grid[4].

[3] N. Kerszberg, P. Suryanarayana. *RSC Adv.* 2015, **5**, 43810–43814.
[4] G. Gui, J. Li, J. Zhong. *Phys. Rev.* 2009, **80**, 167402.

S3. Band structures of highly strained graphene

Figure S2 displays the band structures of graphene unit cells under 20, 25, and 30% applied tensile uniaxial strain in the armchair and zigzag directions. The band gaps reported in the main article (Figure 2) and below in Table S7 are obtained from the band structures and are defined as the energy gaps between the highest fully or partially-occupied electronic band and the lowest unoccupied band. In the case of structures D and F of Figure S2 one can see that here the Fermi level is not at the Dirac point, and thus the highest-occupied band is only partially occupied.

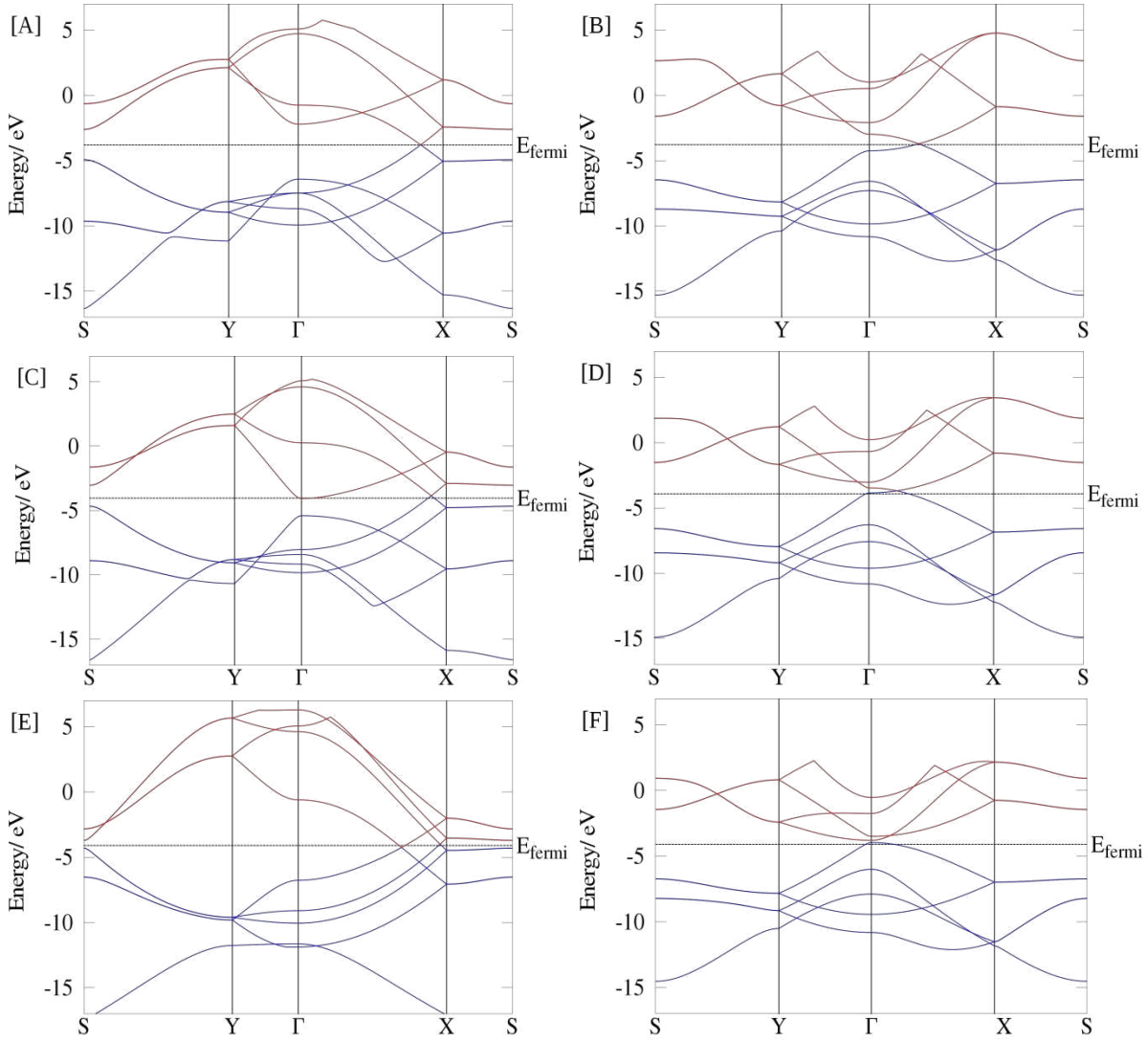

Figure S2. Band structures of highly-strained graphene unit cells: 20% armchair (A) and zigzag (B); 25% armchair (C) and zigzag (D); and 30% armchair (E) and zigzag (F).

S4. Interaction energies in the TiO_2/graphene system

Table S8. Interlayer interaction energies (with binding energies in brackets) and interlayer spacings obtained in this work and in several published systems (see references).

System	Method	Interaction Energy			Interlayer Spacing (Å)
		Per cell (eV)	Per carbon atom (eV)	Per unit area (mJ m^{-2})	
This work, 6 atomic layers TiO_2	PBE + D (CP2K)	-1.35 (-2.40)	-0.019 (-0.033)	-0.11 (-0.20)	2.90
This work, 9 atomic layers TiO_2	PBE + D (CP2K)	-1.67 (-3.24)	-0.023 (-0.045)	-0.14 (-0.26)	2.76
This work, 6 atomic layers TiO_2, alternative orientation, 8 x 5 graphene	PBE + D (CP2K)	-3.67 (-4.55)	-0.023 (-0.028)	-0.14 (-0.18)	2.90
Computational rutile (110)/graphene system (9 atomic layers TiO_2)[2]	LDA + U (VASP)	-1.69	-0.023	-0.14	2.75
Computational anatase (101)/graphene system[5]	LDA + U (CASTEP)	-1.49	-0.050	-0.29	2.57
Computational anatase (101)/graphene system[6]	PBE + D (CRYSTAL 14)	-1.25	-0.042	-0.24	2.84
	PBE + D (Quantum Espresso)	-1.01	-0.034	-0.19	2.97
	B3LYP-D*	-1.44	-0.048	-0.28	2.84
	HSE06-D2	-1.33	-0.044	-0.26	2.77
	vdw-DF2	-0.95	-0.032	-0.18	3.05
Computational graphite system (this work)	PBE + D	n/a	-0.044	-0.27	3.35
Computational graphite system[7]	PBE + D	n/a	-0.051	-0.31	3.35
Computational graphite system[8]	VdW-DF	n/a	-0.050	-0.31	3.59
Computational graphite system[9]	LDA	n/a	-0.024	-0.15	3.33
Experimental multilayer graphene system[10]	TEM	n/a	-0.035	-0.21	n/a

[5] X. Li, H. Gao and G. Liu, *Computational and Theoretical Chemistry*, 2013, **1025**, 30-34.
[6] L. Ferrighi, G. Fazio and C. Di Valentin, *Adv. Mater. Interf.*, 2016, **3**, 1500624.
[7] I. V. Lebedeva, A. A. Knizhnik, A. M. Popov, Y. E. Lozovik and B. V. Potapkin, *Phys. Chem. Chem. Phys.*, 2011, **13**, 5687-95.
[8] E. Ziambaras, J. Kleis, E. Schröder and P. Hyldgaard, *Phys. Rev. B*, 2007, **76**, 155425.
[9] S. Lebègue, J. Harl, T. Gould, J. G. Ángyán, G. Kresse and J. F. Dobson, *Phys. Rev. Lett.*, 2010, **105**, 196401.
[10] L. X. Benedict, N. G. Chopra, M. L. Cohen, A. Zettl, S. G. Louie and V. H. Crespi, *Chem. Phys. Lett.*, 1998, **286**, 490-496.

S5. Density of states for the 6-atomic-layer rutile (110)/graphene composite system

Figure S3 shows the projected density of states (PDoS) data for the 6-atomic-layer rutile (110) slab with and without the presence of graphene. Unlike the 9-atomic-layer composite system (Figure 5 in the main text), there is no significant interaction in the TiO_2 forbidden region between graphene and rutile (110), nor any shift in the positions of the titanium bands above the conduction band of TiO_2. The only noteworthy change in the structure is the appearance of carbon bands in the band gap of TiO_2.

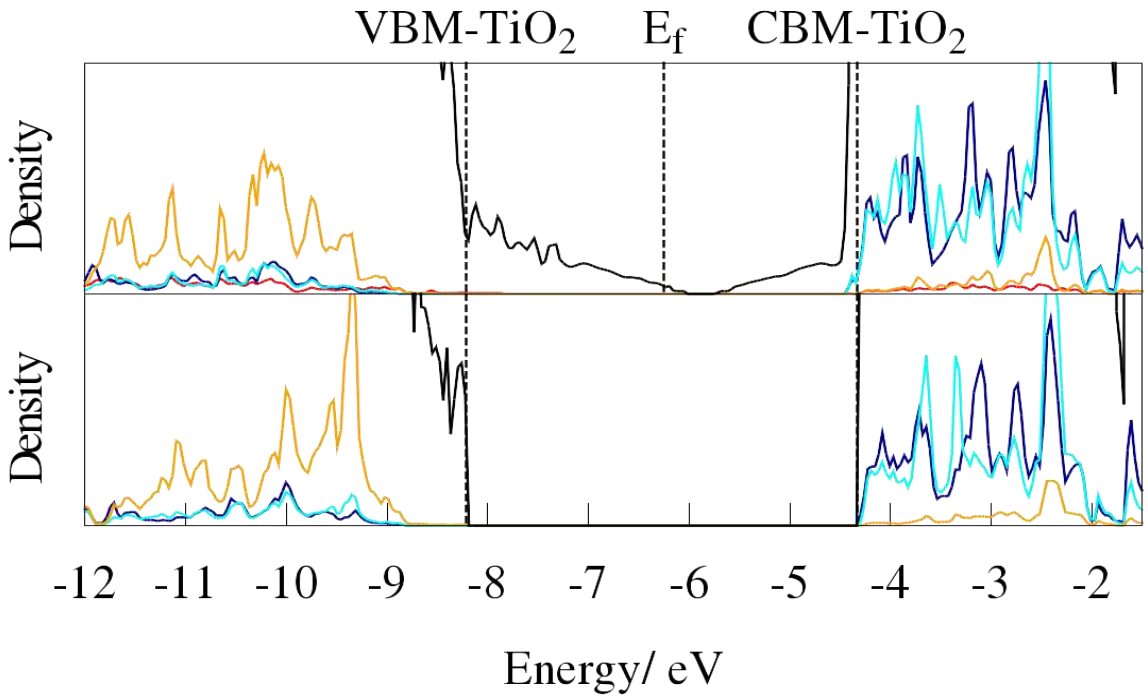

Figure S3. PDoS plot of the 6-atomic-layer rutile (110) slab (bottom) and its composite with graphene (top). The total DoS is shown in black, the projections shown are: carbon (red); 2-coordinated oxygen (orange); 5-coordinated titanium (dark blue); and 6-coordinated titanium (cyan). The dashed lines show the VBM and CBM of the rutile (110) slab, in addition to the Fermi level of the composite as a whole.

S6. Charge density difference in the rutile (110)/graphene composite system

Figure S4 shows the spatial charge density difference between the composite systems and the isolated TiO_2 and graphene systems, for our two TiO_2 slab sizes. In both cases there is a pattern of charge migration across the interface from graphene to rutile, with the magnitude of charge transfer across the interface (0.01 electrons per carbon atom) comparable to what has been seen in similar studies using DFT+U methods (0.007-0.03 electrons per C atom).[2,5,11] Additional evidence for charge transfer from graphene to rutile is seen in the positioning of the Fermi level (Figures 6-7 in the main text), as it lies below the Dirac point by almost 0.5 eV, which is slightly less than that observed in the previous calculations of this interface.[2,5] Both our work and the previous research clearly show that some spontaneous charge transfer from graphene to rutile occurs upon formation of this composite system.

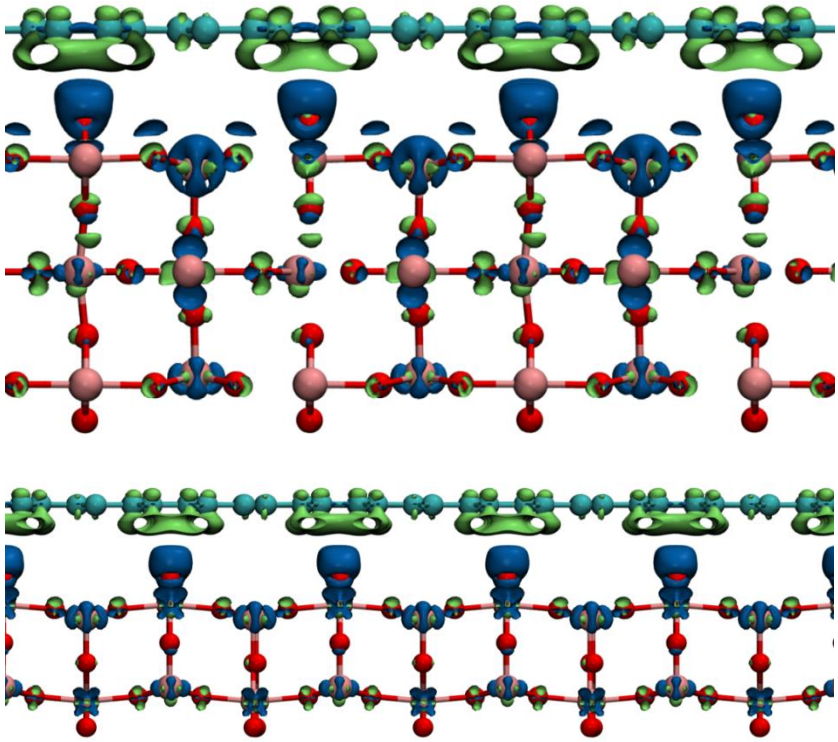

Figure S4. Spatial charge density differences in composites containing the 9 atomic layer (top) and 6 atomic layer (bottom) rutile (110), at isosurface values of 10^{-3} electrons $Bohr^{-3}$.

[11] N. Yang, Y. Liu, H. Wen, Z. Tang, H. Zhao, Y. Li and D. Wang, *ACS Nano*, 2013, **7**, 1504-1512.

S7. Band structures of the rutile (110) and graphene components

Figure S5 shows the band structures of the isolated graphene and the 9-atomic-layer rutile (110) components of the TiO_2/graphene composite. The band structures for the components of the composite show the same characteristic shape as parts the combined composite, such as the flat TiO_2 bands and the more dispersed graphene bands, with the Dirac point appearing away from the Γ point. Comparing the two band structures with the full composite (Figure 7 in the main text) shows that there is little change to the band structure upon formation of the composite.

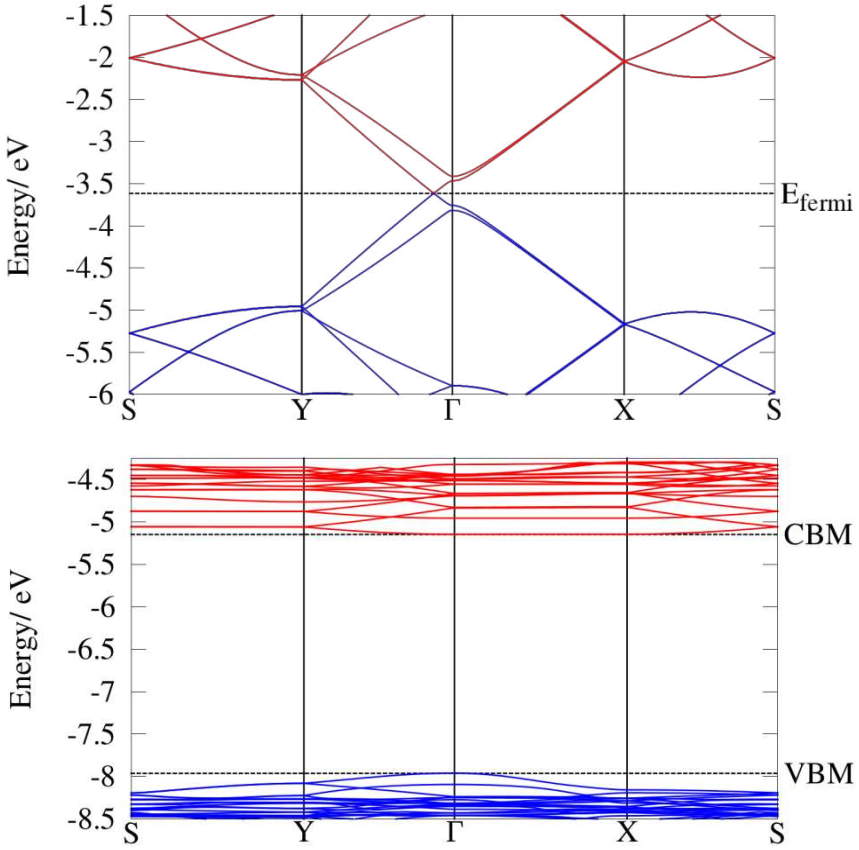

Figure S5. Band structures of the graphene (top) and the 9-atomic-layer rutile (110) (bottom) components of the rutile (110)/graphene composite. In both cases the geometries are those adopted in the composite cell.

S8. Example of CP2K input file for rutile (110)/graphene system

Listed here are the input settings used in the geometry optimisation of the 9 atomic layer rutile (110)/graphene composite unit cell, using the HSE06 hybrid functional with the CP2K software package, as described in the main article. Special care must be taken with the value of `EPS_SCHWARZ` (which defines the integral screening parameter) when incorporating graphene in the calculation, as this number needs to be sufficiently small to prevent numerical instabilities from causing the SCF procedure to fail. Smaller values will increase the number of integrals used in the calculation of Hartree-Fock exchange, but subsequently raise the demand on computing resources. Smaller basis sets are typically better conditioned, and thus do not need such a small value of `EPS_SCHWARZ` to avoid convergence issues.

```
&GLOBAL
  PROJECT Rutile-110-Graphene-Unit-HSE06-3layer
  RUN_TYPE GEO_OPT
  PRINT_LEVEL LOW
&END GLOBAL

 &MOTION
  &GEO_OPT
   OPTIMIZER CG
   &CG
   &END CG
  &END GEO_OPT
 &END MOTION

&FORCE_EVAL
  METHOD Quickstep
 &DFT
  WFN_RESTART_FILE_NAME Rutile-110-Graphene-Unit-HSE06-3layer-
RESTART.wfn
  &AUXILIARY_DENSITY_MATRIX_METHOD
  &END AUXILIARY_DENSITY_MATRIX_METHOD
    &MGRID
      CUTOFF 600
      NGRIDS 5
    &END MGRID
    &QS
     EPS_PGF_ORB 1.0E-20
    &END QS
    &SCF
      SCF_GUESS RESTART
      EPS_SCF 1.0E-6
      MAX_SCF 51
      &OT
        MINIMIZER CG
        PRECONDITIONER FULL_SINGLE_INVERSE
        ENERGY_GAP 0.1
      &END OT
      &OUTER_SCF
         EPS_SCF 1.0E-6
         MAX_SCF 20
      &END OUTER_SCF
    &END SCF
    &XC
      &XC_FUNCTIONAL
```

```
       &PBE
        SCALE_X 0.0
        SCALE_C 1.0
       &END PBE
       &XWPBE
        SCALE_X -0.25
        SCALE_X0 1.0
        OMEGA 0.11
       &END XWPBE
      &END XC_FUNCTIONAL
      &HF
       FRACTION 0.25
       &SCREENING
        EPS_SCHWARZ 1.0E-7
       &END SCREENING
       &INTERACTION_POTENTIAL
        POTENTIAL_TYPE SHORTRANGE
        OMEGA 0.11
       &END INTERACTION_POTENTIAL
       &MEMORY
        MAX_MEMORY 4000
        EPS_STORAGE_SCALING 0.1
       &END MEMORY
      &END HF
     &VDW_POTENTIAL
         DISPERSION_FUNCTIONAL PAIR_POTENTIAL
         &PAIR_POTENTIAL
            TYPE DFTD2
            REFERENCE_FUNCTIONAL PBE
         &END PAIR_POTENTIAL
      &END VDW_POTENTIAL
    &END XC
  &END DFT
  &SUBSYS
     &KIND O
       BASIS_SET DZVP-MOLOPT-GTH-q6
       POTENTIAL GTH-PBE-q6
       AUX_FIT_BASIS_SET FIT3
     &END KIND
     &KIND Ti
       BASIS_SET DZVP-MOLOPT-SR-GTH-q12
       POTENTIAL GTH-PBE-q12
       AUX_FIT_BASIS_SET FIT11
     &END KIND
     &KIND C
       BASIS_SET DZVP-MOLOPT-GTH-q4
       POTENTIAL GTH-PBE-q4
       AUX_FIT_BASIS_SET FIT3
     &END KIND
  &CELL
A    13.058000000    0.000000000    0.000000000
B     0.000000000   14.975000000    0.000000000
C     0.000000000    0.000000000   30.000000000
  &END CELL
  &COORD
<System_Structure>
  &END COORD
  &END SUBSYS
&END FORCE_EVAL
```